Poly(amidoamine) Dendrimer−Methotrexate Conjugates: The Mechanism of Interaction with Folate Binding Protein

Mallory A. van Dongen,[†] Rahul Rattan,[‡,∥] Justin Silpe,[‡] Casey Dougherty,[†] Nicole L. Michmerhuizen,[⊥] Margaret Van Winkle,[⊥] Baohua Huang,[∥] Seok Ki Choi,[∥] Kumar Sinniah,[⊥] Bradford G. Orr,[§,∥] and Mark M. Banaszak Holl*,[†,‡,∥]

[†]Departments of Chemistry, [‡]Biomedical Engineering, [§]Physics, and [∥]the Michigan Nanotechnology Institute for Medicine and Biological Sciences, University of Michigan, Ann Arbor, Michigan 48109, United States
[⊥]Department of Chemistry, Calvin College, Grand Rapids, Michigan 49546, United States

S Supporting Information

ABSTRACT: Generation 5 poly(amidoamine) (G5 PAMAM) methotrexate (MTX) conjugates employing two small molecular linkers, G5-(COG-MTX)$_n$, G5-(MFCO-MTX)$_n$ were prepared along with the conjugates of the G5-G5 (D) dimer, D-(COG-MTX)$_n$, D-(MFCO-MTX)$_n$. The monomer G5-(COG-MTX)$_n$ conjugates exhibited only a weak, rapidly reversible binding to folate binding protein (FBP) consistent with monovalent MTX binding. The D-(COG-MTX)$_n$ conjugates exhibited a slow onset, tight-binding mechanism in which the MTX first binds to the FBP, inducing protein structural rearrangement, followed by polymer−protein van der Waals interactions leading to tight-binding. The extent of irreversible binding is dependent on total MTX concentration and no evidence of multivalent MTX binding was observed.

KEYWORDS: PAMAM dendrimer, methotrexate, multivalent binding, polymer/protein interactions
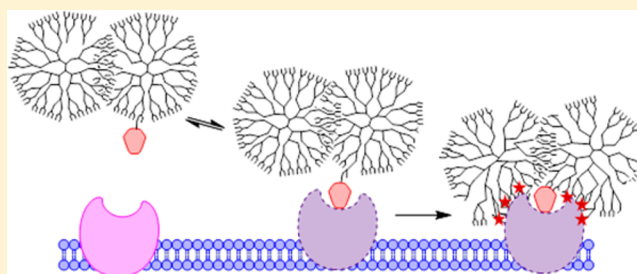
INTRODUCTION

Multivalent drug-polymer conjugates, in which multiple copies of a drug are covalently attached to a polymeric scaffold either directly or through linker chemistry, are a highly studied pathway to improve therapeutic index.[1−7] In particular, conjugation of methotrexate (MTX) to poly(amidoamine) (PAMAM) dendrimer has been extensively studied, with over 100 related publications since 2002.[8−19] Acetylated, neutral G5 PAMAM has been of particular interest as a drug delivery vector because of its narrow polydispersity index (PDI), low toxicity and immunogenicity, and molecular weight (MW) of about 30 kDa that allows it to solubilize multiple hydrophobic ligands while still being small enough to diffuse through tissue for cell-level targeting.[20] MTX is a structural derivative and competitive inhibitor of folic acid (FA);[21] therefore, it was proposed that MTX conjugates may also be able to provide increased binding and uptake when multivalently displayed on a polymer scaffold.[12,14,16] Recent work by van Dongen, Banaszak Holl et al. has shown that multivalent G5 PAMAM folic acid conjugates (G5-(COG-FA)$_n$) bind to FBP via a slow onset, tight-binding interaction[22−25] in which FA first binds, the protein structure rearranges,[23,26] and then polymer−protein van der Waals forces provide the final tight-binding interaction (Figure 1a).[27] In other words, the tight-binding of polymer conjugate does not arise from multiple FA-protein interactions, and a single FA-FBP interaction suffices to initiate the polymer−protein interaction. This has also been described as a "lock and key" interaction by Licata and

Tkachenko, wherein FA serves as a strong key to unlock van der Waals polymer/protein interactions.[28] For such protein−ligand polymer interactions, a particularly interesting aspect to explore is key strength. When interacting with FBP, MTX is a "weak key" as compared to FA. As measured by surface plasmon resonance, the K_D of MTX to FBP is ∼2 times greater than that of FA. This difference arises from a 40% decrease in k_a coupled with a 30% increase in k_d.[14] However, several orders of magnitude in higher concentrations of MTX are required to trigger the observed conformational change of the FBP.[29,30]

The studies in this paper are designed to answer the following questions. (1) Do the G5 PAMAM MTX conjugates interact with FBP via the slow-onset, tight binding mechanism? (2) Can the weaker MTX still initiate the strong polymer−protein van der Waals interactions? (3) Can greater polymer size (i.e., dimer G5 with MW of ∼60 000 Da vs monomer G5 MW of ∼30 000 Da) give rise to increased total polymer−protein interaction and offset the impact of the "weaker key"? (4) Does the weaker binding of MTX allow G5-MTX$_n$ to achieve multivalent binding, as previously proposed?[12,14,16] (5) What is the impact of tuning "key strength" by varying the linker connecting the key to the polymer?
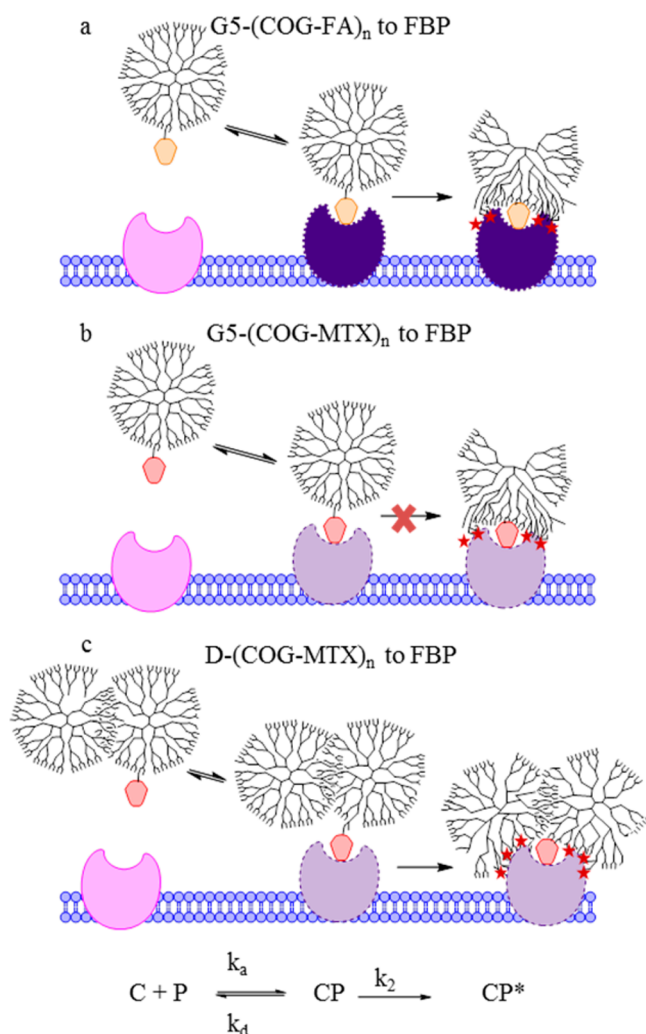
Figure 1. Mechanism of binding for (a) G5-(COG-FA) conjugates to FBP mimics slow, tight binding. (b) G5-(COG-MTX) conjugates cause less protein conformational change to the polymer and do not irreversibly bind. (c) D-(COG-MTX) conjugates also demonstrate slow, tight binding. Abbreviations: COG = cyclooct-1-yn-3-glycolic acid, C = polymer conjugate, P = protein.

In this work, we examine the individual and combined impacts of vector size variation, linker chemistry, and dendrimer valency by synthesizing monomeric and dimeric G5 conjugates with well-defined numbers of MTX attached to the dendrimer through two linker systems. Recent protocols developed to isolate precise ratio ligand-to-dendrimer conjugates from stochastic distributions[27,31,32] were employed to create conjugates with narrow, well-defined populations. Surface plasmon resonance (SPR) and isothermal titration calorimetry (ITC) were employed to measure the impact of these parameters on G5-MTX$_n$ to FBP binding.

■ EXPERIMENTAL SECTION

Materials. All chemicals and materials were purchased from Sigma-Aldrich or Fisher Scientific and used as received unless otherwise specified. Ethylene diamine (EDA) core G5 PAMAM dendrimer was purchased from Dendritech and purified into monomer (G5; average molecular weight of 27.7 kDa by GPC, with a range of 26−30 kDa as determined by mass spectrometry) and dimer (D; average molecular weight of 53 kDa by GPC)

samples as previously described.[33] Click-Easy MFCO-*N*-hydroxysuccinimide was purchased from Berry & Associates Synthetic Medicinal Chemistry. γ-Azido-MTX was synthesized as described previously.[34] Cyclooct-1-yn-3-glycolic acid (COG) was synthesized as previously reported.[27]

Preparation of G5-COG$_{4.7(avg)}$ Conjugate. Conjugates were prepared using G5 via EDC-NHS coupling. In brief, 240.4 mg of amine-terminated monomer G5 was dissolved to 0.16 μM in deionized water (DI). A total of 12.0 mg of COG ligand was activated by dissolving to 10.5 μM in acetonitrile with 2.65 equiv of EDC and 2.78 equiv of *N*-hydroxysuccinimide and stirring for 2 h. The activated COG solution was added dropwise via syringe pump (∼0.33 mL/min) to the dendrimer solution and allowed to stir overnight. The product was purified using Amicon Ultra Centrifugal units, 10 kDa cutoff membranes, 2 PBS washes, and 4 DI washes. A total of 170.6 mg of white solid was isolated via lyophilization. The material was fully acetylated (100% of remaining primary amines converted to acetyl groups, henceforth termed "Ac") by redissolving in anhydrous methanol (0.19 μM), adding 450 equiv of triethylamine and 360 equiv of acetic anhydride, and stirring for 4 h. The product mixture was purified by centrifugation and isolated by lyophillization. G5-COG$_{4.7(avg)}$ was characterized by rp-UPLC and ^{1}H NMR (Supporting Information Figures S4−S5).

Preparation of G5-MFCO$_{2.0(avg)}$ Conjugate. Amine-terminated G5 PAMAM was dissolved to 0.16 μM in DI. Click-Easy MFCO-*N*-hydroxysuccinimide was activated by dissolving to 10.5 μM in acetonitrile and added dropwise via syringe pump (∼0.33 mL/min) to the dendrimer solution. The solution was stirred overnight. The product was purified using Amicon Ultra Centrifugal units, 10 kDa cutoff membranes, two PBS washes, and four DI washes. Product was isolated via lyophillization. The material was then fully acetylated as described above. G5-MFCO$_{2.0(avg)}$ was characterized by rp-UPLC and ^{1}H NMR (Supporting Information Figures S6−S7).

Preparation of D-COG$_{4.8(avg)}$ Conjugate. G5-G5 dimer COG conjugates were prepared using EDC/NHS coupling according to the procedures outlined for G5 PAMAM monomer. A total of 100.8 mg of dimer and 5 equiv of COG ligand were employed. D-COG$_{4.8(avg)}$ was characterized by rp-UPLC and ^{1}H NMR (Supporting Information Figures S8−S9).

Preparation of D-MFCO$_{6.2(avg)}$ Conjugate. G5 PAMAM dimer MFCO conjugates were prepared using Click-Easy MFCO-*N*-hydroxysuccinimide according to the procedures outlined for G5 PAMAM monomer. A total of 115.5 mg of dimer and 6.4 equiv of MFCO ligand were employed. D-MFCO$_{6.2(avg)}$ was characterized by rp-UPLC and ^{1}H NMR (Supporting Information Figures S10−S11).

Isolation of Precise Ratio G5-COG$_x$, G5-MFCO$_x$, D-COG$_x$, and D-MFCO$_x$ Conjugates (x = 0−3, 3+, or 4+) (Figure 2). G5 PAMAM monomer and dimer dendrimers with precise ratios of COG or MFCO ligands per dendrimer were isolated via rp-HPLC according to modified literature procedures.[35] Briefly, multiple injections of the stochastic conjugate containing an average ligand/dendrimer ratio were performed with a C18 column and a water/acetonitrile gradient with 0.1% TFA. Eluted fractions were collected and combined to obtain G5 PAMAM monomer samples with precise COG/dendrimer ratio of 0−5 (G5-COG$_x$, x = 1−5) or precise MFCO/dendrimer ratio of 0−4 (G5-MFCO$_x$, x = 1−4, 5+). G5 PAMAM dimer samples with precise COG/dimer ratio of 0−2 (D-COG$_x$, x = 1−2, 3+) were also obtained. Products were purified using PD-10 desalting protocols with DI as the equilibration buffer, dissolved in 10×
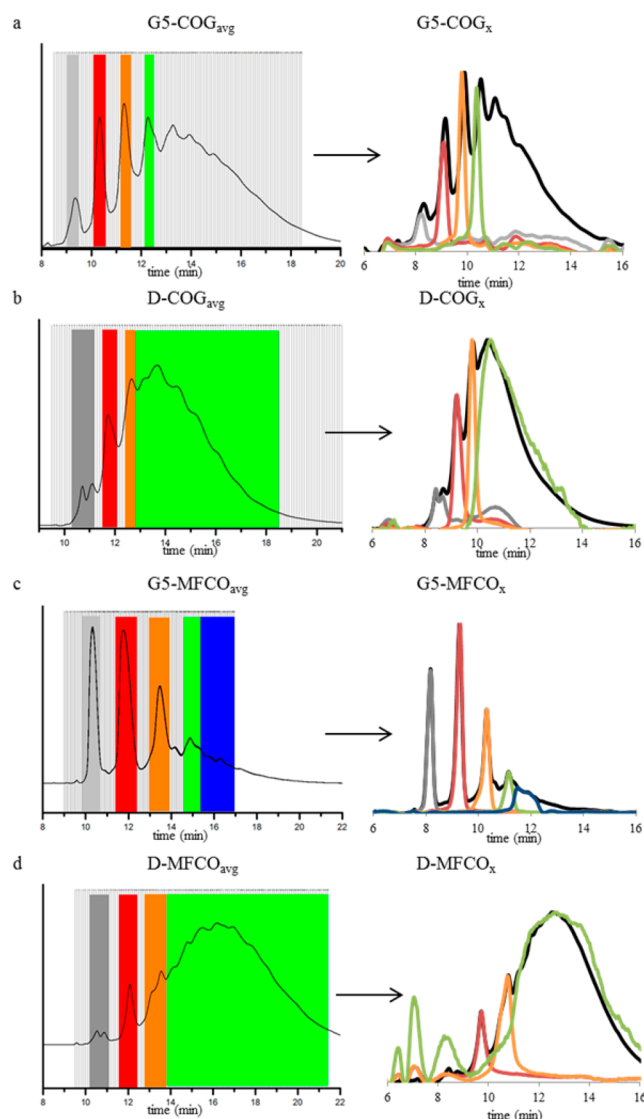
Figure 2. (left) rp-HPLC traces and fractions collected from average conjugations of (a) G5-COG$_x$, (b) D-COG$_x$, (c) G5-MFCO$_x$, and (d) D-MFCO$_x$.(right) rp-UPLC traces of average conjugation (black) and each collected fraction.

PBS, and then lyophilized to dry. Samples were characterized by UPLC and ^{1}H NMR. Curve fitting of UPLCs by Igor Pro was performed to provide yield, purity, and HPLC MFCO and COG averages.

Synthesis of G5-(COG-MTX)$_n$, G5-(MFCO-MTX)$_n$, D-(COG-MTX)$_n$, D-(COG-MTX)$_{4.0(avg)}$, and G5-(MFCO-MTX)$_{4.0(avg)}$ Conjugates. Dendrimers with defined numbers of covalently bound methotrexates were synthesized via click reaction of precise ratio G5-COG$_n$, G5-MFCO$_n$, D-COG$_n$, or D-MFCO$_n$ conjugates and γ-azido-MTX. Briefly, dendrimer conjugates were dissolved in DMSO to 40 mM with respect to the click ligand, and a 10-fold excess of γ-azido-MTX (40 mM in DMSO) was added. Solutions were agitated for 48 h, then diluted to 2.5 mL with 10× PBS and purified using PD-10 desalting columns (gravity protocols). Further purification was performed via 10 kDa cutoff dialysis against DI with 16 media changes. Lyophilized samples were characterized by ^{1}H NMR spectroscopy and UPLC. Curve fitting of UPLC chromatograms provided yield, purity, and MTX averages (Supporting Information Figures S12–S16).

Methods. *High Performance Liquid Chromatography.* Isolation of precise ligand/dendrimer ratio conjugates was achieved using a Waters 600 Controller, Waters 2707 Autosampler, and Waters 2998 Photodiode Array running Empower 2 Software, additionally equipped with a Waters Fraction Collector III on a Phenomenex Jupiter 300 Å C18 Prep Column (21.2 × 150 mm, 5 μm particles). The weak solvent (Solvent A) was HPLC grade Water with 0.1% TFA, and the strong solvent (Solvent B) was HPLC grade Acetonitrile with 0.1% TFA. The gradient employed at 16 mL/min was as follows: 2.1 min load step at 95%A/5%B, 3.9 min gradient to 80%A/20% B, 15 min gradient to 65%A/35%B, 5 min gradient to 55%A/45% B, followed by 3 min was at 20%A/80%B, then equilibrating at starting conditions for 5 min before next injection. The stochastically synthesized dendrimer conjugates were dissolved to 20 mg/mL concentration and 910 μL injections were used. Five-second fractions were collected starting at 9 min 30 s into each run for a total of 120 fractions. Analytical chromatograms were collected on a Waters Acquity UPLC equipped with a scaled method using a Phenomenex Jupiter 4.6 × 100 mm column.

LC Peak Fitting. UPLC chromatograms were fit with Gaussian peaks using Igor Pro Version 6.0.3.1 software. Peak widths within a chromatogram were kept constant.

Nuclear Magnetic Resonance Spectroscopy. NMR experiments were performed on Varian VNMRS 500 and Varian MR400 instruments. ^{1}H NMR spectra were obtained used 10 s preacquisition delays and a total of 64 scans. All sample solutions were set to a dendrimer concentration of 5 mg/mL in deuterium oxide.

Isothermal Titration Calorimetry. All experiments were performed on a Nano ITC Standard Volume from TA Instruments (Lindon, UT). G5-(MFCO-MTX)$_{4.0(avg)}$ (70, 200, 400 μM with respect to MTX), G5-(MFCO-MTX)$_{4+}$ (313.3 μM with respect to MTX), free MTX (200 μM), and FBP (4 μM) solutions were prepared in pH 7.4 PBS buffer and then degassed for 25 min. Before loading, the syringe and cell were each rinsed with degassed PBS buffer three times. The reference cell of the ITC was refilled with degassed, nanopure water every 2 days. After flushing the sample cell with buffer, the syringe was filled with the MTX solution and the sample cell was filled with the FBP solution. Using ITCRun software the parameters of the ITC were set (stir rate, 250 rpm; injection interval, 1000 s; injection volume, 12 μl; injections, 20; temperature, 25 °C) and the instrument was allowed to auto equilibrate before starting the titrations. Controls were performed by injecting the same concentration of MTX conjugates into PBS buffer. These control runs were then subtracted from the experimental runs to account for heat from mixing or dilution and were analyzed using TA NanoAnalyze software (ver 2.4.1). The area under each peak was integrated and the resulting data was modeled using an independent model fit with variables ΔH, binding stoichiometry (n), and K_A.

Surface Plasmon Resonance. SPR experiments were conducted in a Biacore X instrument (Pharmacia Biosensor AB). An immobilized folate binding protein (FBP) chip was prepared following the instrument prompted protocols, using a solution of 0.2 M EDC and 0.05 M NHS as an activating solution, 1 mg/mL FBP solution as the immobilization solution, and ethanolamine as the deactivation solution. The chip was characterized using free FA and methotrexate solutions ranging from 0.1 to 2 mM. Conjugate samples were dissolved in fresh pH 7.4 HBS-EP buffer (Fisher Scientific) at 60 μM and serially

Scheme 1. Conjugation of (a) Monomer G5 to COG, (b) G5−G5 Dimer[a] to COG via EDC/NHS Coupling, (c) Monomer G5 to MFCO, and (d) G5−G5 Dimer[a] to MFCO by Direct Conjugation Followed by Full Acetylation of the Dendrimer Surface with Acetic Anhydride
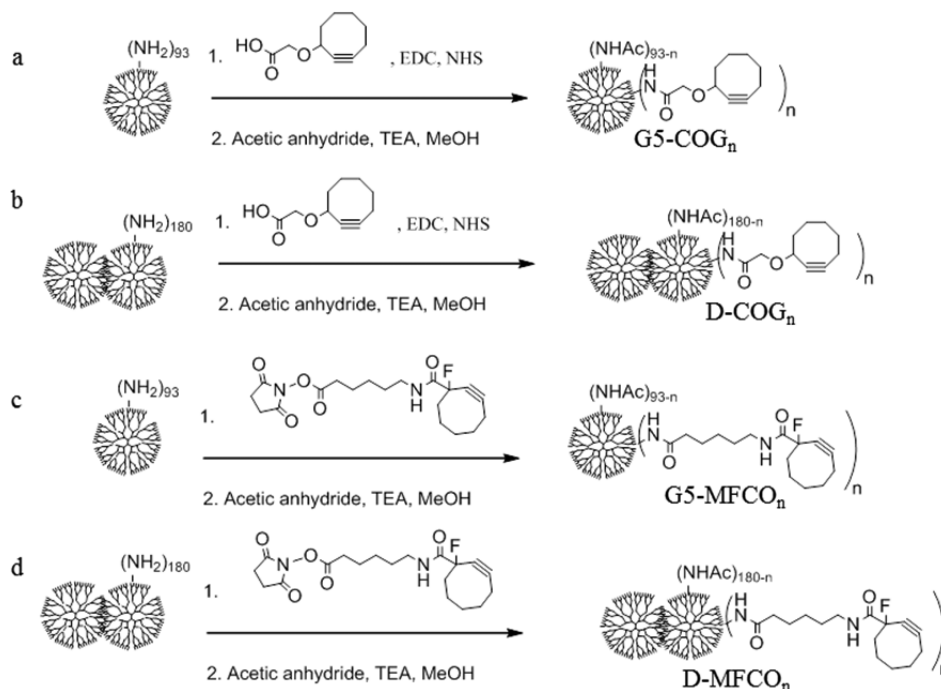
[a]Dimer is notated as "D".

diluted to 10, 5, 2.5, and 1.25 μM in buffer. Runs were multichannel, (FC1-FC2) at 10 μL/min. The system was allowed to equilibrate at the beginning of each run for no less than 300 s, followed by a 2 min, 30 μL (50−5−5−5 via bubble method) injection. The system was monitored for no less than 500 s per injection. Between each run, the chip was washed with a 5 μL injection of pH 1.5 buffer to remove bound materials followed by a prime step prior to the next injection.

■ RESULTS AND DISCUSSION

A major challenge to detailed scientific understanding of multivalent dendrimer binding mechanisms has been the presence of trailing generations (G1−G4) and oligomers (dimers, trimers, etc.) in the dendrimer conjugates studied. Recently, we have developed methods for gram-scale isolation of PAMAM materials as a function of dendrimer size[33] and milligram-scale isolation as a function of conjugate valency.[31,32,35−37] These methods create an opportunity to improve valency control of multivalent conjugates and improve the ability to analyze the binding mechanism of previously developed multicomponent mixtures. Here, we directly compare PAMAM monomer and dimer MTX conjugates using SPR- and ITC-based measurements of binding characteristics. These experiments probe the effect of vector size both as a design principle for its own sake and to attribute binding behaviors to monomer and dimer, which were present in the materials employed in previous SPR studies.[12,16] In addition to valency, the influence of linker length/flexibility/hydrophobicity for the system was also explored.

Preparation of Dendrimer Conjugates Containing Precise Ratios of COG and MFCO Click Ligands (Scheme 1, Figure 2). G5 PAMAM dendrimer monomer (G5) and dimer (D) were isolated from commercially available material as

previously described.[33] Stochastic conjugations to fluorinated (MFCO) and nonfluorinated (COG) ring strain promoted click chemistry ligands were performed via amide coupling reactions resulting in materials containing a distribution of ligand/dendrimer ratios ranging from 0 to 13 covalently attached ligands per dendrimer. Overall reaction yields of the white solids ranged from 37 to 43%. Peak fitting of rp-UPLC chromatograms was employed to determine the average ligand-to-dendrimer ratio for each sample.[35−37] These stochastic mixtures were then isolated by semipreparative rp-HPLC following previously reported protocols.[32] The purity of the isolated, precise ratio ligand-to-dendrimer conjugates range from 90 to 100% (as defined by ligand/dendrimer ratio dispersity). In addition to the precise ligand/dendrimer ratio materials, samples containing a high *average* number of MFCO ligands (G5-MFCO$_{6.6(avg)}$ and D-MFCO$_{5.3(avg)}$) and a high average of COG ligands (D-COG$_{6.2(avg)}$) were also obtained. Importantly, these samples contain no unfunctionalized ($x = 0$) or monofunctional ($x = 1$) materials, making them good controls for the observation of multivalent (e.g., chelation or statistical rebinding) effects. A summary of all isolated materials can be found in Table 1. These rp-HPLC methods are versatile and have been successfully employed to isolate precise ratio ligand/dendrimer conjugates for both monomer and dimer PAMAM and using three different ligands to date. The presumed mechanism allowing this isolation protocol is a favorable interaction between the conjugated, hydrophobic ligand and the reverse-phase C18 column. The MFCO ligand, which contains a longer carbon chain in addition to the fluorine on the cyclooctyne, results in significantly higher resolution than the shorter COG ligand. This is illustrated in Figure 2, panels a and c, where G5-MFCO$_{2.0(avg)}$ has baseline resolution between $n = 0$ and 1, and $n = 1$ and 2 samples (Figure 2c), whereas G5-COG$_{4.7(avg)}$ has peak overlap for all peaks, even n

Table 1. Summary of Isolated, Precise Ratio Cycloalkyne/Dendrimer Conjugates

vector	ligand	target valency	UPLC average	UPLC purity
monomer	COG	0	0.0	100%
monomer	COG	1	1.1	100%
monomer	COG	2	1.9	90%
monomer	COG	3	2.8	93%
dimer	COG	0	0.0	100%
dimer	COG	1	1.1	91%
dimer	COG	2	2.0	100%
dimer	COG	3+	6.2	n/a
monomer	MFCO	0	0.0	100%
monomer	MFCO	1	1.0	100%
monomer	MFCO	2	1.9	91%
monomer	MFCO	3	3.0	99%
monomer	MFCO	4+	6.6	n/a
dimer	MFCO	0	0.0	100%
dimer	MFCO	1	1.1	100%
dimer	MFCO	2	2.1	100%
dimer	MFCO	3+	5.3	n/a

= 0 and $n = 1$ (Figure 2a). The difference between the $x = 1$ and $x = 2$ peak centers is 0.64 min for the G5-COG conjugates compared to 1.02 min for the MFCO conjugates. The improved resolution likely arises from the greater hydrophobicity of the longer chain resulting in greater interaction with the C18 stationary phase, leading to increased retention as a function of number of ligands. The increased resolution is repeated in the dimer conjugates; however, the resolution of both dimer species is less than the corresponding monomer. As the time difference in peak centers for $x = 1, 2$ is nearly identical between the monomer and dimer for both ligands (0.59 and 1.04 min for dimer conjugated to COG and MFCO, respectively), the reduced resolution is the result of the increased peak width of the dimer species (arising from a broader MW distribution of branching defects[33]). Better rp-HPLC resolution allows for the isolation of higher ratio materials, increased yield of all conjugates, and increased purity of resulting samples.

Synthesis of Dendrimer/MTX Conjugates (Scheme 2). The conjugate samples, containing G5 monomer or dimer conjugated to precise numbers ($x = 0-3$) or high average (3+ or 4+) numbers of COG or MFCO, were then allowed to react with γ-azido-MTX. Click reactions efficiencies ranged from 79 to 100% with mass recoveries over 95%. A detailed analysis of each sample's fractional composition is summarized in Table 2. Click efficiencies were approximately equal for monomer and dimer conjugates and for MFCO and COG.

Isothermal Titration Calorimetry (ITC) (Supporting Information Figure S1). Because of undesired interactions of the MFCO conjugates with the SPR surface (vide infra), the binding of G5-(MFCO-MTX)$_n$ conjugates to FBP was measured by ITC. The stochastically conjugated monomer G5-(MFCO-MTX)$_{4(avg)}$ sample displayed endothermic binding (Supporting Information Figure S1a). This indicates that binding between the conjugate and protein can occur, but there is an energetic cost. By way of contrast, there was no observable binding between the isolated high average G5-(MFCO-MTX)$_{4.4}$ sample, which contains only dendrimer clicked to 3 or more MTX. One interpretation of these results would be that the flexibility and hydrophobicity of the MFCO linker cause it to fold into the interior regions of the G5 dendrimer. Consequently, the energetic penalty to hydrate the ligand and allow for MTX/protein interaction is significantly higher, which negatively impacts the enthalpy of binding. Because the lower average sample shows some interaction with the protein, it is possible that there is cooperativity within the MFCO linkers that further block the MTX from interacting with the protein in the higher average sample.

Surface Plasmon Resonance Measurement of Binding (Figures 3 and S2). Weak, reversible binding for G5-(COG-MTX)$_n$ ($n = 0.9, 1.9, 2.9$) to surface immobilized FBP was observed at all concentrations tested. The control samples (fully acetylated monomer and dimer with no MTX) had similar binding to both chips, which when subtracted gave relatively flat chromatograms (Figure 3a and e). By way of contrast, all three tested valencies for the monomer show both a dendrimer and total MTX concentration dependent binding with the FBP
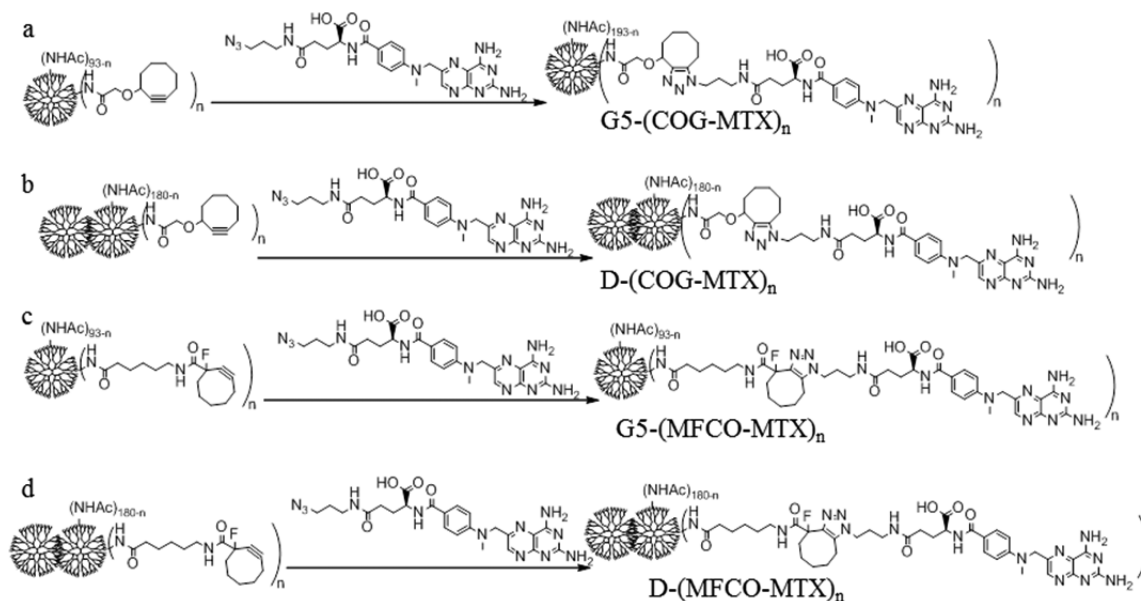
Scheme 2. Click of Precisely Defined G5-COG$_x$, G5-MFCO$_x$, D-COG$_x$, and D-MFCO$_x$ Conjugates to γ-Azido-MTX

Table 2. Quantitative Summary of Click Products

| vector	ligand	target valency	HPLC average of MTX	click yield (%)	% of "n" MTX				
					$n = 0$	$n = 1$	$n = 2$	$n = 3$ (+)	$n = 4+$
monomer	COG	0	0.0	n/a	100	0	0	0	0
monomer	COG	1	0.9	90	10	90	0	0	0
monomer	COG	2	1.9	85	0	14	78	7	0
monomer	COG	3	2.9	79	0	3	18	66	13
dimer	COG	0	0.0	n/a	100	0	0	0	n/a
dimer	COG	1	1.1	100	0	89	11	0	0
dimer	COG	2	2.0	100	0	0	100	0	0
dimer	COG	3+	6.0	n/a	0	0	3	97	n/a
monomer	MFCO	0	0.0	n/a	100	0	0	0	0
monomer	MFCO	1	1.0	100	0	100	0	0	0
monomer	MFCO	2	1.7	87	6	15	79	0	0
monomer	MFCO	3	2.7	89	0	0	35	62	3.1
monomer	MFCO	4+	4.4	n/a	0	0	0	21	79
dimer	MFCO	0	0.0	n/a	100	0	0	0	n/a
dimer	MFCO	1	1.1	100	0	95	5	0	0
dimer	MFCO	2	2.1	100	0	0	91	9	0
dimer	MFCO	3+	4.4	n/a	0	0	0	100	n/a
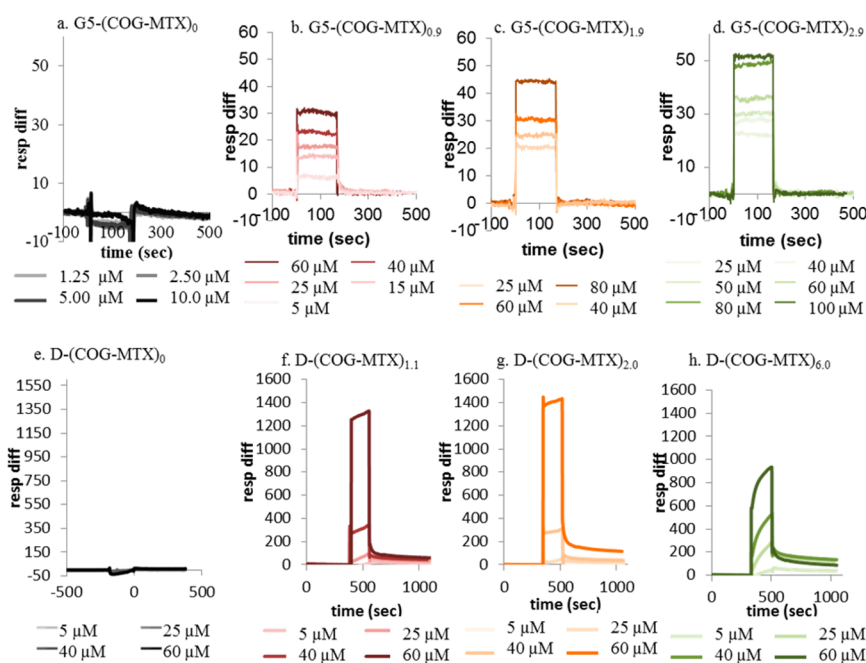
Figure 3. SPR results of all click products. Color gradients represent least concentrated (light) to most concentrated (dark) injections. (a) G5 (acetylated control), (b) G5-(COG-MTX)$_{0.9}$, (c) G5-(COG-MTX)$_{1.9}$, (d) G5-(COG-MTX)$_{2.9}$, (e) D (acetylated control), (f) D-(COG-MTX)$_{1.1}$, (g) D-(COG-MTX)$_{2.0}$, (h) D-(COG-MTX)$_{6.0}$.

surface. Figure 4 reveals that G5-(COG-MTX)$_n$ exhibits greater association phase binding (i.e., higher signal) as valency increases (Figure 4a). For all injections, the signal initially rose sharply at the beginning of the injection and quickly reached equilibrium between association and dissociation. This is indicative of a fast-on, fast-off relationship. In other words, in Figure 1b k_a and k_d are both large and rapid as compared to k_2, and strong irreversible binding does not occur. At the end of the injection, all chromatograms quickly return to baseline, confirming the fast dissociation of all bound species. This indicates that even the divalent (66%) and trivalent species (13%) in the G5-(COG-MTX)$_{2.9}$ experience only monovalent binding to the FBP surface. There is no multivalency effect for increasing the MTX valency (n) for G5-(COG-MTX)$_n$. The data were fit to the

expression $R = R_{max}[C]/([C] + K_d)$ to yield the apparent K_d values of $6.3 \pm 0.4 \times 10^{-5}$ M, $7.4 \pm 0.7 \times 10^{-5}$ M, and $8.6 \pm 1.1 \times 10^{-5}$ M for G5-(COG-MTX)$_{0.9}$, G5-(COG-MTX)$_{1.9}$, and G5-(COG-MTX)$_{2.9}$, respectively (all fits used a common R_{max} value of 67, see below). However, when the data is plotted as a function of total MTX concentration it fits well to a single binding isotherm (Figure 4b). Fitting the concentration dependent data for all three samples to a single expression resulted in an R_{max} value of 67 ± 8 and a K_d value of $7.6 \pm 1.8 \times 10^{-5}$ M.

The D-(COG-MTX)$_n$ data show a different trend. Total concentration of MTX does not explain the trend in the binding phase (Figure 4d) and a higher average number of MTX ligands per dendrimer actually show less surface binding for a given concentration of MTX. However, there is a binding phase signal
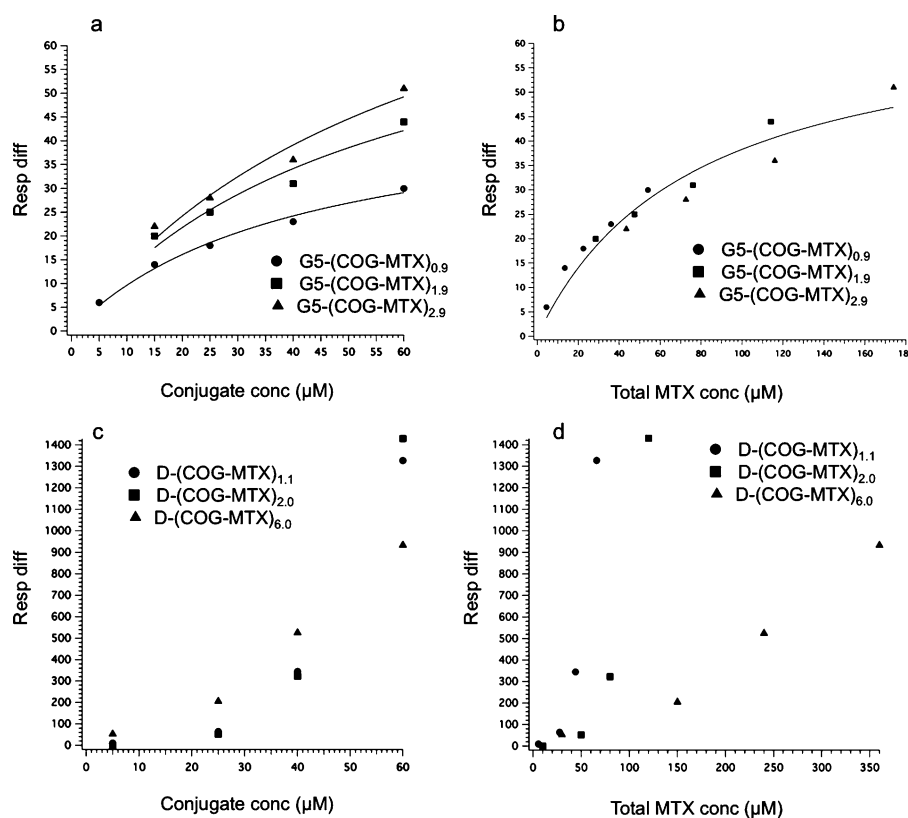
Figure 4. Saturation of SPR signal during the binding phase as a function of (a) conjugate concentration for monomer samples, (b) total MTX concentration for monomer samples, (c) conjugate concentration for dimer samples, and (d) total MTX concentration for dimer samples. The data in panels a and b is fit to the expression $R = R_{max}[C]/([C] + K_d)$ for an A + B $\leftrightarrows$ C equilibrium.

dependence based on dendrimer concentration (Figure 4c). The data indicate that at the concentrations tested, D-(COG-MTX)$_n$ with an MTX valency of at least $n = 1$, an association/dissociation equilibrium (k_a and k_d as represented schematically in Figure 1c) is not reached during sample injection (Figure 3f–h). At equilibrium, higher MTX valencies would be expected to have more total binding due to statistical rebinding effects. However, at these concentrations a single MTX/FBP interaction (Figure 3e–f) is sufficient to establish the van der Waals interaction (k_2 in Figure 1) between the dimer and protein. The amount of binding observed is therefore approximately equal for equivalent dendrimer concentrations (Figure 4c). With a stronger binder, such as FA (Figure 1a), equilibrium is established at lower concentrations and the total binding becomes dependent on total ligand concentration (vide infra, Figures 5–6). Therefore, a dependence on MTX valency cannot be established for the D-(COG-MTX)$_n$ case. The higher concentrations (to achieve equilibrium during the injection) that would have allowed full exploration of the likely sigmoidal functional response were not tested due to conjugate solubility. Quantitative fits of the type shown for Figure 4a and b are not possible. However, it can be concluded that the interaction must be "keyed" by conjugated MTX, as there is negligible accumulation observed in the acetylated control (D) sample (Figure 3e). In this case, possible MTX valency dependent effects on binding, including statistical rebinding and chelation, do not lead to the observed greater overall conjugate binding.

As indicated by Supporting Information Figure S3, both G5-(MFCO-MTX)$_n$ and D-(MFCO-MTX)$_n$ have a negative overall signal in injection/association phase as a result of nonspecific
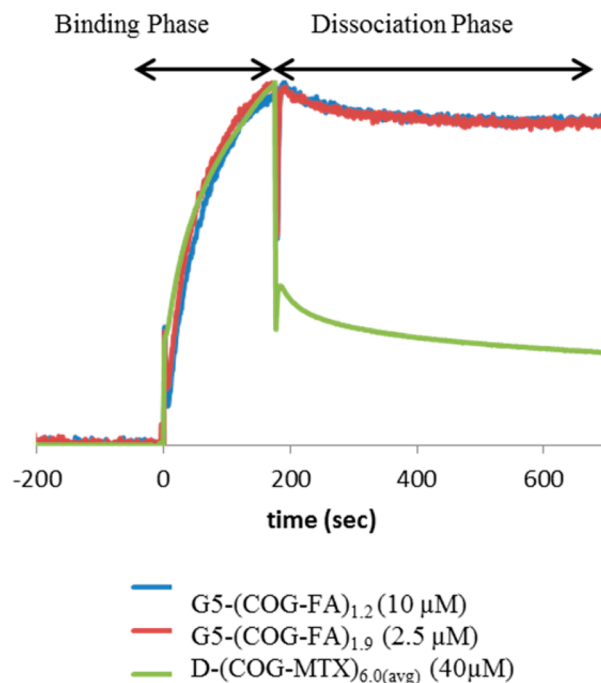
Figure 5. Comparison of the SPR sensograms of a D-(COG-MTX)$_{6.0}$ sample to two different G5-(COG-FA)$_n$ samples, with total signal normalized.

interactions with the chip surface in the control flow cell (FC2). Further analysis of these data was not pursued.
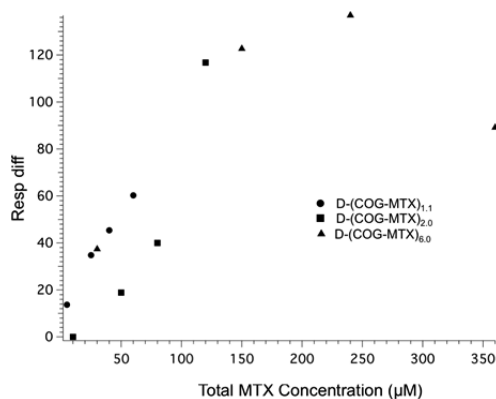
Figure 6. Amount of bound material D-(COG-MTX)$_n$ after 500 s of dissociation is dependent on absolute MTX concentration and FBP density, not MTX valency.

The MTX conjugate data described above can be compared to a study of monomeric G5-(COG-FA)$_n$ (n = 0, 1, 1.2, 1.9, 2.7) conjugates by van Dongen, Banaszak Holl et al. that indicated greatly increased avidity via SPR with a significant portion of bound material not dissociating over the time scale of the experiment.[27] Because this observation held true for even a purely monovalent (folic acid-to-dendrimer ratio of 1) sample, it was concluded that the observation of increased avidity was due to the sum of weak van der Waals interactions between the dendrimer and protein surface (Figure 1a). This interaction is initiated by an interaction between a conjugated FA and the FBP, which causes a conformational change in the protein exposing a more hydrophilic surface to interact with the dendrimer (schematically represented as a color change in Figure 1). MTX, as a structurally modified competitive inhibitor of FA, may undergo a similar interaction with the FBP. However, although the experiments here were performed on surfaces with both higher protein densities and higher conjugate concentrations, a similar avidity increase for monomer G5-(COG-MTX)$_n$ conjugates was not observed at even the highest valency tested (n =3). Previous studies indicated only a ∼2 fold increased binding of free FA as compared to free MTX;[14] therefore, the significant reduction in binding strength of G5-(COG-MTX)$_n$ compared to G5-(COG-FA)$_n$ is most likely due to a reduction in polymer/protein interactions. MTX is a "weak" key to the FBP "lock", and the structural rearrangement of the protein is not large enough to establish van der Waals interactions for a polymer of the same size. For the MTX case, there are indications of enhanced avidity for the dimer samples (D-(COG-MTX)$_n$). However, when comparing the overall shape of the G5-(COG-FA)$_n$ and D-(COG-MTX)$_{6.0(avg)}$ sensograms (Figure 5) it becomes clear that there are some fundamental differences. For the G5-(COG-FA)$_n$ samples, nearly all materials that bound (to a protein density dependent saturation point) remained permanently attached to the surface. By contrast, a large percentage of the D-(COG-MTX)$_n$ material quickly dissociates after the conjugate flow has stopped. This indicates that k_d is much larger for the MTX conjugates as compared to the FA conjugates, that k_2 is much smaller (Figure 1a and c), or that for some binding sites steric contraints prevent achieving the magnitude of polymer/protein interaction that leads to irreversible binding. These three factors may also act in concert. The D-(COG-MTX)$_n$ conjugates show a dendrimer concentration, not MTX concentration, dependent association to the protein surface (Figure 4c). The absolute signal, when compared

to that of the monomer/MTX conjugates, is approximately 10× higher in the dimer species at equivalent molar concentrations. A 2-fold increase may be expected by this technique due to doubling in mass. This leads to a qualitative assumption that more binding occurs in dimer samples as compared to monomer samples for equivalent total MTX concentrations. This 5-fold increase over the "expected" association signal is likely caused by the larger mass and radius of the dimer[33] increasing the van der Waals interactions between the dendrimer/FBP (i.e., an increase in k_2 from negligible in the monomer data to contributing for dimer conjugates). Chelate-type binding between multiple MTX and one or more FBP is not observed, in even the high-valency dimer samples. Figure 6 indicates that the amount of irreversibly bound material (defined as the portion of signal remaining after 500 s of dissociation) is dependent only on the absolute MTX concentration in solution and not on conjugate valency. If chelate binding was responsible for the irreversible binding, the bivalent and high valent samples would be expected to have enhanced binding as compared to the monovalent samples at similar MTX concentrations. Instead, the amount of strongly bound material has a linear dependence on MTX concentration prior to reaching a saturation at ∼120 response units.

Previous SPR studies on PAMAM-COG-MTX conjugates (containing mixtures of dimer and monomer) indicated both monovalent and multivalent binding occurred for stochastic valencies of n = 5 and n = 10.[16] The present work indicates that the origin of the portion of binding assigned as "multivalent" arose from the presence of dimers conjugated to 3 or more MTX. The dendrimer material in previous studies contained ∼14% dimer[33] and assuming a Poisson distribution, the "multivalent" portion of the n = 5 and 10 samples would be 13% and 14%, respectively.

■ CONCLUSIONS

New chromatographic methods have enabled the examination of vector molecular weight effects (monomer vs dimer), linker system effects (COG vs MFCO), and valency effects on the highly studied drug delivery system of PAMAM dendrimer conjugated to methotrexate. The answers to the questions posed at the start of the paper can now be addressed: (1) The monomer G5 PAMAM-MTX conjugates show none of the irreversible binding previously attributed to multivalency for stochastic conjugate synthesized using commercial dendrimer containing oligomers of G5. The dimer G5 PAMAM-MTX conjugates do show irreversible binding, including D-MTX$_1$, which cannot bind via a multivalent MTX mechanism. The slow-onset, tight-binding mechanism is consistent with these observations. (2 and 3) Although the weaker MTX does not initiate sufficient structural change for the irreversible binding to occur between FBP and monomer G5, the larger dimer of G5 interacting with the protein is able to generate a large enough interaction for irreversible binding. (4) It has been suggested that weaker linkers could provide longer surface diffusion times and, thus, potentially allow multivalent ligand binding.[28] We did not observe multivalent MTX binding for these samples. (5) We attempted to tune key strength by varying the linker; however, this resulted in a number of changes including differential solution binding enthalpy likely related to hydrophobicity and undesired binding to control surfaces.

In summary, the preparation of controlled valency monomer G5 and dimer G5−G5 conjugates, demonstrate that multivalency is not an active binding mechanism for these conjugates and a slow, onset−tight binding mechanism is proposed that is

consistent with mechanistic hypotheses for the analogous FA conjugates[27] and the mechanistic proposals of Licata and Tkachenko.[28]

■ ASSOCIATED CONTENT

Ⓢ Supporting Information

ITC results, individual flow cell data, SPR sensograms, ^{1}H NMR graphs, and UPLC chromatograms. This material is available free of charge via the Internet at http://pubs.acs.org.

■ AUTHOR INFORMATION

Corresponding Author

*E-mail: mbanasza@umich.edu.

Notes

The authors declare no competing financial interest.

■ ACKNOWLEDGMENTS

■ REFERENCES

(1) Cloninger, M. J.; Bilgiçer, B.; Li, L.; Mangold, S. L.; Phillips, S. T.; Wolfenden, M. L. Multivalency. In *Supramolecular Chemistry*; John Wiley & Sons, Ltd: 2012.

(2) Liu, S.; Maheshwari, R.; Kiick, K. L. Polymer-Based Therapeutics. *Macromolecules* 2009, 42, 3−13.

(3) Soliman, G. M.; Sharma, A.; Maysinger, D.; Kakkar, A. Dendrimers and miktoarm polymers based multivalent nanocarriers for efficient and targeted drug delivery. *Chem. Commun.* 2011, 47, 9572−9587.

(4) Mintzer, M. A.; Grinstaff, M. W. Biomedical applications of dendrimers: a tutorial. *Chem. Soc. Rev.* 2011, 40, 173−190.

(5) Kono, K.; Liu, M.; Fréchet, J. M. J. Design of Dendritic Macromolecules Containing Folate or Methotrexate Residues. *Bioconjugate Chem.* 1999, 10, 1115−1121.

(6) Svenson, S.; Tomalia, D. A. Dendrimers in biomedical applications—reflections on the field. *Adv. Drug Delivery Rev.* 2005, 57, 2106−2129.

(7) Menjoge, A. R.; Kannan, R. M.; Tomalia, D. A. Dendrimer-based drug and imaging conjugates: design considerations for nanomedical applications. *Drug Discovery Today* 2010, 15, 171−185.

(8) Huang, B. H.; Otis, J.; Joice, M.; Kotlyar, A.; Thomas, T. P. PSMA-Targeted Stably Linked "Dendrimer-Glutamate Urea-Methotrexate" as a Prostate Cancer Therapeutic. *Biomacromolecules* 2014, 15, 915−923.

(9) Quintana, A.; Raczka, E.; Piehler, L.; Lee, I.; Myc, A.; Majoros, I.; Patri, A.; Thomas, T.; Mulé, J.; Baker, J., Jr. Design and Function of a Dendrimer-Based Therapeutic Nanodevice Targeted to Tumor Cells Through the Folate Receptor. *Pharm. Res.* 2002, 19, 1310−1316.

(10) Gillies, E. R.; Fréchet, J. M. J. Dendrimers and dendritic polymers in drug delivery. *Drug Discovery Today* 2005, 10, 35−43.

(11) P. Thomas, T.; Joice, M.; Sumit, M.; E. Silpe, J.; Kotlyar, A.; Bharathi, S.; Kukowska-Latallo, J.; R. Baker, J.; Ki Choi, S. Design and In vitro Validation of Multivalent Dendrimer Methotrexates as a Folate-targeting Anticancer Therapeutic. *Current Pharmaceutical Design* 2013, 19, 6594−6605.

(12) Thomas, T. P.; Huang, B.; Choi, S. K.; Silpe, J. E.; Kotlyar, A.; Desai, A. M.; Zong, H.; Gam, J.; Joice, M.; Baker, J. R. Polyvalent Dendrimer-Methotrexate as a Folate Receptor-Targeted Cancer Therapeutic. *Mol. Pharmaceutics* 2012, 9, 2669−2676.

(13) Gurdag, S.; Khandare, J.; Stapels, S.; Matherly, L. H.; Kannan, R. M. Activity of Dendrimer−Methotrexate Conjugates on Methotrexate-Sensitive and -Resistant Cell Lines. *Bioconjugate Chem.* 2006, 17, 275−283.

(14) Li, M.-H.; Choi, S. K.; Thomas, T. P.; Desai, A.; Lee, K.-H.; Kotlyar, A.; Banaszak Holl, M. M.; Baker, J. R., Jr. Dendrimer-based multivalent methotrexates as dual acting nanoconjugates for cancer cell targeting. *Eur. J. Med. Chem.* 2012, 47, 560−572.

(15) Goonewardena, S. N.; Kratz, J. D.; Zong, H.; Desai, A. M.; Tang, S.; Emery, S.; Baker, J. R.; Huang, B. Design considerations for PAMAM dendrimer therapeutics. *Bioorg. Med. Chem. Lett.* 2013, 23, 2872−2875.

(16) Silpe, J. E.; Sumit, M.; Huang, B.; Kotlyar, A.; van Dongen, M. A.; Banaszak Holl, M. M.; Orr, B. G.; Choi, S. K. Avidity Modulation of Folate-Targeted Multivalent Dendrimers for Evaluating Biophysical Models of Cancer Targeting Nanoparticles. *ACS Chem. Biol.* 2013, 8, 2063−2071.

(17) Jiang, Y. Y.; Tang, G. T.; Zhang, L. H.; Kong, S. Y.; Zhu, S. J.; Pei, Y. Y. PEGylated PAMAM dendrimers as a potential drug delivery carrier: in vitro and in vivo comparative evaluation of covalently conjugated drug and noncovalent drug inclusion complex. *J. Drug Targeting* 2010, 18, 389−403.

(18) Gurdag, S.; Khandare, J.; Stapels, S.; Matherly, L. H.; Kannan, R. M. Activity of dendrimer-methotrexate conjugates on methotrexate-sensitive and -resistant cell lines. *Bioconjugate Chem.* 2006, 17, 275−283.

(19) Wu, G.; Barth, R. F.; Yang, W. L.; Kawabata, S.; Zhang, L. W.; Green-Church, K. Targeted delivery of methotrexate to epidermal growth factor receptor-positive brain tumors by means of cetuximab (IMC-C225) dendrimer bioconjugates. *Mol. Cancer Ther.* 2006, 5, 52−59.

(20) Baker, J. R. Why I believe nanoparticles are crucial as a carrier for targeted drug delivery. *WIREs: Nanomed. Nanobiotechnol.* 2013, 5, 423−429.

(21) Chen, C.; Ke, J. Y.; Zhou, X. E.; Yi, W.; Brunzelle, J. S.; Li, J.; Yong, E. L.; Xu, H. E.; Melcher, K. Structural basis for molecular recognition of folic acid by folate receptors. *Nature* 2013, 500, 486−489.

(22) Williams, J. W.; Duggleby, R. G.; Cutler, R.; Morrison, J. F. The inhibition of dihydrofolate reductase by folate analogues: Structural requirements for slow- and tight-binding inhibition. *Biochem. Pharmacol.* 1980, 29, 589−595.

(23) Szedlacsek, S. E.; Duggleby, R. G. Kinetics of slow and tight-binding inhibitors. In *Methods in Enzymology*; Daniel, L. P., Ed.; Academic Press: Salt Lake City, UT, 1995; Vol. Vol. 249, pp 144−180.

(24) Ross, P. D.; Subramanian, S. Thermodynamics of protein association reactions: forces contributing to stability. *Biochemistry* 1981, 20, 3096−3102.

(25) Van Oss, C. J.; Good, R. J.; Chaudhury, M. K. The role of van der Waals forces and hydrogen bonds in "hydrophobic interactions" between biopolymers and low energy surfaces. *J. Colloid Interface Sci.* 1986, 111, 378−390.

(26) Holm, J.; Lawaetz, A. J.; Hansen, S. I. Ligand binding induces a sharp decrease in hydrophobicity of folate binding protein assessed by 1-anilinonaphthalene-8-sulphonate which suppresses self-association of the hydrophobic apo-protein. *Biochem. Biophys. Res. Commun.* 2012, 425, 19−24.

(27) van Dongen, M. A.; Silpe, J. E.; Dougherty, C.; Kanduluru, A. K.; Choi, S. K.; Orr, B. G.; Low, P. S.; Banaszak Holl, M. M. Avidity Mechanism of Dendrimer-Folic Acid Conjugates. *Mol. Pharmaceutics* 2014, 11, 1696−1706.

(28) Licata, N. A.; Tkachenko, A. V. Kinetic Limitations of Cooperativity-Based Drug Delivery Systems. *Phys. Rev. Lett.* 2008, 100, 158102.

(29) Bruun, S. W.; Holm, J.; Hansen, S. I.; Andersen, C. M.; Nørgaard, L. A Chemometric Analysis of Ligand-Induced Changes in Intrinsic Fluorescence of Folate Binding Protein Indicates a Link Between Altered Conformational Structure and Physico-Chemical Characteristics. *Appl. Spectrosc.* 2009, 63, 1315−1322.

(30) Holm, J.; Hansen, S.; Høier-Madsen, M. Ionic Charge, Hydrophobicity and Tryptophan Fluorescence of the Folate Binding Protein Isolated from Cow's Milk. *Biosci. Rep.* 2001, 21, 305−313.

(31) Mullen, D. G.; Borgmeier, E. L.; Desai, A. M.; van Dongen, M. A.; Barash, M.; Cheng, X.-m.; Baker, J. R.; Banaszak Holl, M. M. Isolation and Characterization of Dendrimers with Precise Numbers of Functional Groups. *Chem.—Eur. J.* 2010, 16, 10675−10678.

(32) van Dongen, M. A.; Vaidyanathan, S.; Banaszak Holl, M. M. PAMAM Dendrimers as Quantized Building Blocks for Novel Nanostructures. *Soft Matter* **2013**, *9*, 11188−11196.

(33) van Dongen, M. A.; Desai, A.; Orr, B. G.; Baker, J. R., Jr.; Banaszak Holl, M. M. Quantitative analysis of generation and branch defects in G5 poly(amidoamine) dendrimer. *Polymer* **2013**, *54*, 4126−4133.

(34) Huang, B.; Desai, A.; Zong, H.; Tang, S.; Leroueil, P. R.; Baker, J. R., Jr. Copper-free click conjugation of methotrexate to a PAMAM dendrimer platfrom. *Tetrahedron Lett.* **2011**, *52*, 1411−1414.

(35) Mullen, D. G.; Fang, M.; Desai, A.; Baker, J. R., Jr.; Orr, B. G.; Banaszak Holl, M. M. A Quantitative Assessment of Nanoparticle-Ligand Distributions: Implications for Targeted Drug and Imaging Delivery in Dendrimer Conjugates. *ACS Nano* **2010**, *4*, 657−670.

(36) Mullen, D. G.; Banaszak Holl, M. M. Heterogeneous Ligand−Nanoparticle Distributions: A Major Obstacle to Scientific Understanding and Commercial Translation. *Acc. Chem. Res.* **2011**, *44*, 1135−1145.

(37) Dougherty, C. A.; Furgal, J. C.; van Dongen, M. A.; Goodson, T., III; Banaszak Holl, M. M. Isolation and Characterization of Precise Dye/Dendrimer Ratios. *Chem.—Eur. J.* **2014**, *20*, 4638−4645.